

## Episodic super-Eddington accretion as a clue to Overmassive Black Holes in the early Universe

ALESSANDRO TRINCA,<sup>1,2,3</sup> ROSA VALIANTE,<sup>2</sup> RAFFAELLA SCHNEIDER,<sup>4,2,3,5</sup> IGNAS JUODŽBALIS,<sup>6</sup> ROBERTO MAIOLINO,<sup>6,7</sup>  
LUCA GRAZIANI,<sup>4,2,3</sup> ALESSANDRO LUPI,<sup>1,8</sup> PRIYAMVADA NATARAJAN,<sup>9,10,11</sup> MARTA VOLONTERI,<sup>12</sup> AND TOMMASO ZANA<sup>4,2,3</sup>

<sup>1</sup>Como Lake Center for Astrophysics, DiSAT, Università degli Studi dell'Insubria, via Valleggio 11, 22100, Como, Italy

<sup>2</sup>INAF/Osservatorio Astronomico di Roma, Via Frascati 33, 00040 Monte Porzio Catone, Italy

<sup>3</sup>INFN, Sezione Roma1, Dipartimento di Fisica, "Sapienza" Università di Roma, Piazzale Aldo Moro 2, 00185, Roma, Italy

<sup>4</sup>Dipartimento di Fisica, "Sapienza" Università di Roma, Piazzale Aldo Moro 2, 00185 Roma, Italy

<sup>5</sup>Sapienza School for Advanced Studies, Viale Regina Elena 291, 00161 Roma, Italy

<sup>6</sup>Kavli Institute for Cosmology, University of Cambridge, Madingley Road, Cambridge CB3 0HA, UK

<sup>7</sup>Cavendish Laboratory, University of Cambridge, 19 JJ Thomson Avenue, Cambridge CB3 0HE, UK

<sup>8</sup>INFN, Sezione di Milano-Bicocca, Piazza della Scienza 3, I-20126 Milano, Italy

<sup>9</sup>Department of Astronomy, Yale University, New Haven, CT 06511, USA

<sup>10</sup>Department of Physics, Yale University, New Haven, CT 06511, USA

<sup>11</sup>Yale Center for Astronomy & Astrophysics, Yale University, New Haven, CT 06520, USA

<sup>12</sup>Institut d'Astrophysique de Paris, Sorbonne Université, CNRS, UMR 7095, 98 bis bd Arago, 75014 Paris, France

### ABSTRACT

Early JWST observations are providing growing evidence for a ubiquitous population of accreting supermassive black holes (BHs) at high redshift, many of which appear overmassive compared to the empirically-derived local scaling relation between black hole mass and host galaxy stellar mass. In this study, we leverage predictions from the semi-analytical Cosmic Archaeology Tool (CAT) to reconstruct the evolutionary pathways for this overmassive BH population, investigating how they assemble over cosmic time and interact with their host galaxies. We find that the large  $M_{\text{BH}} - M_{\text{star}}$  ratios can be explained if light and heavy BH seeds grow by short, repeated episodes of super-Eddington accretion, triggered by major galaxy mergers. On average, we find that BH-galaxy co-evolution starts in earnest only at  $z < 8$ , when  $\simeq 30\%$  of the final galaxy stellar mass has formed outside the massive black hole host. Our model suggests that super-Eddington bursts of accretion last between 0.5 – 3 Myr, resulting in a duty cycle of 1 – 4% for the target BH sample. The boost in luminosity of BHs undergoing super-Eddington accretion helps explaining the luminosity function of Active Galactic Nuclei observed by JWST. At the same time, a large population of these overmassive BHs are predicted to be inactive, with Eddington ratio  $\lambda_{\text{Edd}} < 0.05$ , in agreement with recent observations.

*Keywords:* Galaxies: high-redshift – Galaxies: active - quasars: supermassive black holes - Galaxies: evolution - Accretion, accretion disks

### 1. INTRODUCTION

The James Webb Space Telescope (JWST) has opened a new observational window on the Active Galactic Nuclei (AGNs) population at high-redshift, allowing us to identify and study AGNs via optical and UV diagnostic diagrams even at low masses and low luminosities. Significant progress has been made through deep spec-

troscopic observations, which have revealed the presence of broad H $\alpha$  and H $\beta$  emission lines. Potential contamination due to the presence of outflows in these systems is disfavoured by the lack of detection of a broad counterpart in other bright emission lines, such as the forbidden transition of [OIII]5007 Å, clearly pointing towards the presence of a Broad Line Region (BLR, Maiolino et al. 2024a) and hence an active AGN. These observations have revealed a previously unseen population of intermediate/low luminosity AGNs at  $z > 4$ , and out to  $z \simeq 11$ , with estimated black hole (BH) masses in

the range  $10^6$  to  $10^8 M_\odot$ , and bolometric luminosities  $L_{\text{bol}} \sim (10^{43} - 10^{46}) \text{erg/s}$  (e.g. Übler et al. 2023; Barro et al. 2023; Maiolino et al. 2024b; Harikane et al. 2023; Larson et al. 2023; Oesch et al. 2023; Onoue et al. 2023; Ono et al. 2023; Yang et al. 2023; Leung et al. 2023). These BH masses and luminosities are 2–3 orders of magnitude lower than those inferred for quasars at the same redshifts. In addition, the identification of narrow-line (i.e. type-2, as opposed to type-1 AGNs showing BLR emission) AGNs has been possible using UV and optical high-ionization emission lines (e.g. Scholtz et al. 2023; Mazzolari et al. 2024a; Chisholm et al. 2024). Of paramount importance is the discovery of three AGNs at  $z \geq 10$  (Maiolino et al. 2024a; Bogdán et al. 2024; Kovács et al. 2024) that are pushing our exploration closer to the seeding epoch, thereby enhancing our ability to constrain their origin (e.g. Natarajan et al. 2017; Valiante et al. 2018b,a).

JWST has also revealed a previously unknown population of systems, dubbed “little red dots” (LRDs; Matthee et al. 2024), which consists of very compact sources with a steep, red, rest-frame optical continuum emission, presumably dominated by an obscured AGN component (Greene et al. 2024; Labbe et al. 2023; Furtak et al. 2023, and see also Fujimoto et al. 2022). This interpretation is supported by the detection of broad emission lines, although alternative explanations suggest that their properties could also be attributed entirely to stellar emission (Baggen et al. 2024). The fraction of LRDs hosting an AGN is still debated, with estimates ranging from 20% (Pérez-González et al. 2024) to 80% (Greene et al. 2024), and it strongly depends on the detailed selection function. Conversely, the fraction of type-1 AGNs selected by JWST that exhibit LRD-like colors and slopes is reported to be between 10% and 30% (Hainline et al. 2024; Maiolino et al. 2024b). The LRD population appears to be ubiquitous from  $z \geq 3$  (Barro et al. 2024) to  $z \simeq 9$  (Leung et al. 2023), spanning several orders of magnitude in luminosity (Akins et al. 2024).

These new JWST discoveries imply a very large number density of AGNs at  $z \simeq 4 - 7$  (Maiolino et al. 2024b; Scholtz et al. 2023; Greene et al. 2024; Kocevski et al. 2024; Akins et al. 2024), which is 1 or 2 orders of magnitude larger than the extrapolation of the luminosity function probed by the quasar population (Niida et al. 2020), and higher than the estimated density from deep X-ray observations (Giallongo et al. 2015, 2019). Interestingly, a large fraction of these JWST-detected AGNs appears to be powered by BHs that are overmassive with respect to their host galaxy stellar component, with a BH-to-stellar mass ratio of even up to

$M_{\text{BH}}/M_{\text{star}} \sim 0.1 - 1$  (Maiolino et al. 2024b; Juodžbalis et al. 2024; Pacucci & Loeb 2024; Harikane et al. 2023; Übler et al. 2023; Furtak et al. 2024; Kokorev et al. 2023; Yue et al. 2024b; Bogdán et al. 2024). This is an offset that is at least two orders of magnitudes higher than expected from the local  $M_{\text{BH}} - M_{\text{star}}$  scaling relation (Kormendy & Ho 2013; Reines & Volonteri 2015). This finding has been interpreted in some studies as a result of a large scatter in the BH-stellar mass relation, combined with expected selection effects (Lauer et al. 2007). Luminous and massive BHs, whose emission significantly dominates that of their host galaxy, are more likely to be detected in flux-limited surveys (e.g. Volonteri et al. 2023; Zhang et al. 2023; Li et al. 2024). Measurement uncertainties in estimating the BH and/or stellar masses may also help mitigate the observed offset (Lupi et al. 2024b; King 2024). Recent discoveries of overmassive BHs associated with low-luminosity AGNs, characterized by BH-to-stellar mass ratios closer to unity, provide tentative support for an intrinsic evolution of the  $M_{\text{BH}} - M_{\text{star}}$  relation with redshift (Juodžbalis et al. 2024). Furthermore, the finding that the  $M_{\text{BH}} - \sigma$  relation of these high- $z$  AGNs aligns closer to the local scaling suggests that the offset on the  $M_{\text{BH}} - M_{\text{star}}$  relation is not entirely driven by selection effects. Even if selection biases play a significant role and we are detecting only a tail of the population, the observed overmassive black holes represent a collection of extraordinary objects that are challenging to explain within standard BH evolutionary scenarios.

In this work, we aim to explore the implications of these findings for early BH formation and subsequent growth. In particular, we use a cosmological semi-analytical model, the Cosmic Archaeology Tool (CAT; Trinca et al. 2022, 2023), to address the origin of overmassive BHs at  $4 < z < 6$  and account for their large number densities. We find that both of these properties can be accounted for if BH seeds are permitted to experience short phases of super-Eddington accretion.

The paper is organized as follows. The main features of our model are summarized in Section 2 while CAT predictions for the JWST overmassive BH population are detailed in Section 3. We present the properties of the sample of synthetic overmassive BHs in Section 3.1, showing the evolutionary connection to their host galaxies (Section 3.2) and their predicted growth timescale (Section 3.3). Specifically, we investigate the origin and fate of CAT BH candidates representative of the “dormant” BHs observed by Juodžbalis et al. (2024) at  $z \sim 7$  (Sections 4) and discuss the impact of our findings on the predicted AGN luminosity function (Section 5). Finally, CAT results and their implications are critically

discussed in Section 6 and the main conclusions of this work are presented in Section 7.

## 2. MODELING THE GALAXY-BLACK HOLE CO-EVOLUTION

CAT is a semi-analytical model developed to characterize the formation of the first galaxies and their nuclear BHs, and to follow their subsequent co-evolution in a full cosmological context across cosmic time. Here we summarize the main features of the model, and we refer the reader to the original papers for a more detailed description (Trinca et al. 2022, 2023, 2024).

### 2.1. Dark matter merger trees

CAT relies on the GALFORM semi-analytic model (Parkinson et al. 2008) to reconstruct the hierarchical merger history of a large sample of dark matter halos between  $z = 4$  and  $z = 24$ , with a halo mass resolution corresponding to a virial temperature of  $T_{\text{vir}} = 1200$  K. This enables us to characterize the evolution of a large galaxy sample, representative of the global population, over the broad halo mass range  $M_{\text{halo}} \simeq 10^6 - 10^{14} M_{\odot}$ . CAT is therefore able to resolve the first episodes of star formation, taking place at  $z > 20$  inside molecular-cooling *minihalos* ( $T_{\text{vir}} < 10^4$  K) and to characterize in detail the formation of the first BH seeds that depend on the environmental properties of the host galaxies.

### 2.2. Star formation

Inside a galaxy, the star formation rate (SFR) is computed from the available gas mass,  $M_{\text{gas}}$ , as follows:

$$SFR = f_{\text{cool}} M_{\text{gas}} \epsilon_{\text{SF}} / \tau_{\text{dyn}}, \quad (1)$$

where  $\epsilon_{\text{SF}}$  is the star formation efficiency (a free parameter of the model), and  $\tau_{\text{dyn}} \equiv [R_{\text{vir}}^3 / (GM_{\text{halo}})]^{1/2}$  is the halo dynamical time. The factor  $f_{\text{cool}}$  ranges between 0 and 1 and depends on the halo properties, being = 1 only for atomic cooling halos. In minihalos,  $f_{\text{cool}}$  quantifies the reduced cooling efficiency induced by Lyman–Werner (LW) radiation, in the [11.2 – 13.6] eV energy band, which can photodissociate molecular hydrogen. In these halos  $f_{\text{cool}} < 1$  and depends on the halo virial temperature, redshift, gas metallicity and intensity of the illuminating LW radiation (Valiante et al. 2016; de Bressan et al. 2017; Sassano et al. 2021).

We assume that Population III (PopIII) stars form in pristine/metal poor halos, where the metallicity is  $Z < Z_{\text{crit}} = 10^{-3.8} Z_{\odot}$ , according to a top-heavy distribution in the mass interval  $10 \leq m_* \leq 300 M_{\odot}$ , parametrized by a Larson initial mass function (IMF; Larson 1998):

$$\Phi(m_*) = m_*^{\alpha-1} e^{-m_*/m_{\text{ch}}} \quad (2)$$

where  $\alpha = -1.35$  and the characteristic mass is  $m_{\text{ch}} = 20 M_{\odot}$ . As discussed in (Trinca et al. 2024), the adopted Pop III star formation efficiency is  $\epsilon_{\text{SF}} = 0.15$ . This IMF is stochastically sampled as a function of the effective total stellar mass formed in each star formation episode (Valiante et al. 2016; de Bressan et al. 2017).

In contrast, in halos enriched above the metallicity threshold,  $Z > Z_{\text{crit}}$ , less massive, Population II (PopII), stars are assumed to form according to Eq. 2 with masses in the range  $0.1 \leq m_* \leq 100 M_{\odot}$  and a characteristic mass  $m_{\text{ch}} = 0.35 M_{\odot}$  (de Bressan et al. 2014, 2017). The efficiency of star formation for PopII host halos is assumed to be  $\epsilon_{\text{SF}} = 0.05$ , which has been shown to reproduce various properties of the high-redshift galaxy population, including the SFR density, stellar mass density, and UV luminosity function (Trinca et al. 2022, 2024).

### 2.3. Black hole seeds formation

In this model, we follow the evolution of two seed BH populations: the *light* seeds, remnant of the first generation of massive and metal-free stars (Population III stars), and the *heavy* seeds, originated through the so-called direct collapse scenario that requires specific environmental conditions (see Inayoshi et al. 2020, for a recent review).

In our model, PopIII stars forming in the mass interval  $40 M_{\odot} < m_* < 140 M_{\odot}$  and  $m_* > 260 M_{\odot}$  are assumed to directly collapse into BHs of comparable mass (Heger & Woosley 2002), after a time delay consistent with their stellar progenitor lifetime. The most massive among these Pop III remnant BHs is then considered as a *light* seed settling in the nucleus of its host galaxy thereafter (see Trinca et al. 2022, 2024, for more details).

The population of *heavy* seeds is instead characterized by a mass of  $10^5 M_{\odot}$  and is assumed to form in atomic-cooling halos (ACH,  $T_{\text{vir}} > 10^4$  K) of pristine gas composition ( $Z < Z_{\text{crit}}$ ), to avoid fragmentation of the gas cloud, and illuminated by a LW flux,  $J_{\text{LW}}$ , intense enough to dissociate  $\text{H}_2$  molecules ( $J_{\text{LW}} > J_{\text{crit}}$ ), thus preventing star formation. Here we adopt a threshold value of  $J_{\text{crit}} = 300 \times 10^{-21} \text{ erg s}^{-1} \text{ cm}^{-2} \text{ Hz}^{-1} \text{ sr}^{-1}$  following Trinca et al. (2022). However, the value of this critical threshold,  $J_{\text{crit}}$ , is highly uncertain (see e.g. Inayoshi et al. 2020, for a discussion). We discussed the impact of different  $J_{\text{crit}}$  on heavy seed formation in previous studies, where we investigated the relative role of different seed populations in the assembly of  $z \sim 6$  SMBHs (Valiante et al. 2016; Sassano et al. 2021).

### 2.4. Black hole mass growth

After the formation of the initial BH seed, we follow the growth of these BHs through gas accretion and

mergers across cosmic time. In [Trinca et al. \(2022\)](#) we explored the imprints of different gas accretion regimes on the predicted BH mass and luminosity functions at different epochs. Here we consider two specific accretion scenarios, the Eddington-limited (EL) and super-Eddington (SE) models.

In the reference model, hereafter the Eddington-limited (EL) scenario, the gas accretion rate cannot exceed the Eddington rate and is calculated following the Bondi-Hoyle-Lyttleton formula ([Bondi 1952](#); [Hoyle & Lyttleton 1941](#)):

$$\dot{M}_{\text{BHL}} = \alpha \frac{4\pi G^2 M_{\text{BH}}^2 \rho_{\text{gas}}(r_A)}{c_s^3} \quad (3)$$

where  $c_s$  is the sound speed and  $\rho_{\text{gas}}(r_A)$  the gas density evaluated at the radius of gravitational influence of the BH  $r_A = 2GM_{\text{BH}}/c_s^2$ . The factor  $\alpha$  is a free parameter introduced in the original expression to account for the unresolved enhanced gas density in the inner regions around the BH. We assume here  $\alpha = 90$ , which enables us to reproduce the properties of the high redshift quasar population at  $z \simeq 6 - 7$ .

As an alternative accretion paradigm, which we dub as the super-Eddington (SE) scenario, gas accretion is enhanced during brief periods of time ( $\sim 1 - 5$  Myr) as a consequence of galaxy major mergers, defined as mergers amongst halos whose mass ratio is  $\mu > 1/10$  ([Tanaka & Haiman 2009](#)). During these catastrophic events large inflows of gas may be driven towards the nuclear regions through efficient loss of angular momentum. As a result, the rate at which the gas is accreted onto a BH can be higher than the Eddington limit. We compute this rate as:

$$\dot{M} = \frac{\epsilon_{\text{BH}} M_{\text{gas}}}{\tau_{\text{accr}}} \quad (4)$$

where  $M_{\text{gas}}$  is the gas mass inside the newly formed galaxy,  $\epsilon_{\text{BH}} = 0.017$  and  $\tau_{\text{accr}} = 10$  Myr are the assumed BH accretion efficiency and time-scale, respectively. Simultaneously, we also induce an enhancement of the star formation rate (SFR) of the newly formed galaxy, with respect to the prescription presented in [Eq. 1](#), assuming a star formation time-scale  $\tau_{\text{dyn,SF}} = \tau_{\text{accr}}$ , so that  $SFR = \epsilon_{\text{SF}} M_{\text{gas}} / \tau_{\text{dyn,SF}}$  with  $\epsilon_{\text{SF}} = 0.05$  being the same star formation efficiency adopted in the EL model. We refer the reader to [Pezzulli et al. \(2016\)](#) and [Trinca et al. \(2022\)](#) for a detailed description of the set of free parameters and the model calibration. In the SE scenario, the enhanced accretion is sustained as long as one of the two following conditions is met: the elapsed time interval reaches a value  $\Delta t = \tau_{\text{dyn}}/100$ , or the gas-to-BH mass ratio drops below  $M_{\text{gas}}/M_{\text{BH}} < 10$ . Thereafter, the gas accretion is assumed to proceed again at the BHL rate ([Eq. 3](#)), but assuming  $\alpha = 1$ .

Finally, nuclear BHs can also grow through mergers following the coalescences of their host galaxies. In major mergers, we assume that the two nuclear BHs efficiently sink into the centre of the newly formed galaxy instantaneously merging, within the typical time step of the simulation  $\Delta t \sim 0.5 - 4$  Myr, depending on redshift (cosmic time). Conversely, in minor galaxy mergers ( $\mu < 1/10$ ), only the most massive of the two BHs is considered as the nuclear engine of the resulting galaxy while the subsequent evolution of the least massive one is no longer followed. The timescales for binary BH mergers are uncertain and we note here that our assumption of instantaneous merging is optimistic.

### 2.5. Stellar and AGN feedback

In each galaxy, the time evolution of the available gas mass is affected by radiative and mechanical feedback.

In addition to the photodissociating LW radiation regulating the efficiency of star formation, we account for the effect of photo-heating feedback inducing an increase in the gas temperature that may suppress star formation. This occurs in halos with virial temperatures below the temperature of the intergalactic medium, at a given redshift ([Valiante et al. 2016](#)).

In CAT we assume that the coupling of the gas with the energy released during supernova (SN) explosions and the BH accretion process may deplete the reservoir available to star formation and BH accretion within a galaxy, launching powerful outflows that can extend to galaxy-scales. We describe the gas outflow rate due to the combined effect of SN and AGN mechanical feedback as  $\dot{M}_{\text{ej}} = \dot{M}_{\text{ej,SN}} + \dot{M}_{\text{ej,AGN}}$ , where:

$$\dot{M}_{\text{ej,SN}} = 2E_{\text{SN}}\epsilon_{w,\text{SN}}R_{\text{SN}}(t)/v_e^2 \quad (5)$$

and

$$\dot{M}_{\text{ej,AGN}} = 2\epsilon_{w,\text{AGN}}\epsilon_r(t)\dot{M}_{\text{accr}}c^2/v_e^2. \quad (6)$$

In these equations,  $v_e = \sqrt{2GM/R_{\text{vir}}}$  is the escape velocity of the halo,  $E_{\text{SN}}$  is the explosion energy per SN,  $R_{\text{SN}}(t)$  is the total SN explosion rate and  $\dot{M}_{\text{accr}}$  is the gas accretion rate, computed as in [Eq. 3 \(4\)](#) in the EL (SE) model. The AGN radiative efficiency,  $\epsilon_r$ , is fixed to the typical value of 0.1 ([Shakura & Sunyaev 1973](#)) in the EL model, while in the SE scenario can vary according to the [Madau et al. \(2014\)](#) fitting formula for a BH spin of  $a=0.572$  (see [Trinca et al. 2022](#), for further details). Finally, the SN- and AGN-driven wind efficiencies,  $\epsilon_{w,\text{SN}}$  and  $\epsilon_{w,\text{AGN}}$ , are free parameters of the model and are assumed to be  $1.6 \times 10^{-3}$  and  $2.5 \times 10^{-3}$ , respectively for both the EL and SE models ([Trinca et al. 2022](#)). We do not include specific AGN feedback during super-Eddington phases, which are expected to be associated with the emission of powerful bipolar jets from

the accreting BH. Although the impact of jets remains debated, they might play a significant role in limiting BH growth, especially in smaller galaxies (Regan et al. 2019). However, given the relatively large value assumed in CAT for the coupling parameter  $\epsilon_{w,AGN}$ , episodes of SE growth are very efficient in depleting the gas reservoir in less massive systems.

### 3. A POPULATION OF OVERMASSIVE BLACK HOLES

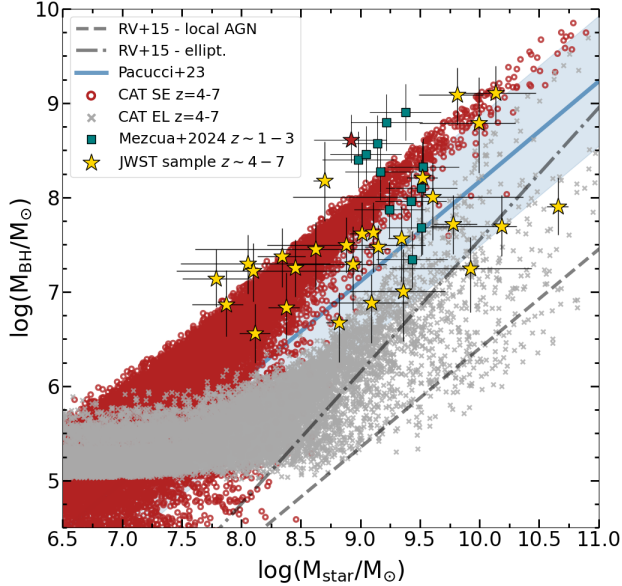


**Figure 1.** Scaling relation between the black hole and the host galaxy stellar mass. grey and red dots represent the BH population predicted between  $4 < z < 7$  by CAT Eddington-limited (EL) and super-Eddington (SE) accretion models, respectively. Model predictions are compared with a sample of overmassive BHs detected in early JWST observations at high redshift  $4 < z < 7$  (yellow stars). The dormant black hole at  $z = 6.67$  identified in the JADES system GN-1001830, analyzed in Section 4, has been highlighted as a red star. We also include the analogous BH population recently detected at cosmic noon ( $1 \lesssim z \lesssim 3$ ) by Mezcuca et al. (2024, teal squares). Black dashed and dash-dotted lines represent the local scaling relation obtained by Reines & Volonteri (2015) for active and passive galaxies, respectively. The blue solid line and shaded region shows instead the high-redshift scaling relation proposed by Pacucci & Loeb (2024) with the inferred scatter.

In Figure 1 we compare the BH vs stellar mass relation predicted by the EL and SE models with the sample of AGNs detected by JWST in low-mass galaxies at redshift  $4 < z < 7$  (Mezcuca et al. 2024, and references therein), aiming to test which evolutionary scenario describes better their estimated properties. We find that the observed massive BH sample is better re-

produced by the SE model, where the simulated systems closely match the region of the  $M_{BH} - M_{star}$  plane occupied by observational data, despite the treatment of BH accretion and feedback in the super-Eddington regime in CAT is relatively simplified (see Section 2). In the EL model, the predicted  $M_{BH}/M_{star}$  ratio is instead significantly lower than observed, more consistent with the local scaling relations for active and passive galaxies (dashed and dot-dashed line, respectively), and the distribution of systems shows a larger scatter, especially at  $M_{star} > 10^{8.5} M_{\odot}$ .

Further, we note that the flattening of the BH mass distribution in the  $M_{BH} \sim 10^5 - 10^6 M_{\odot}$  range is a consequence of the BH accretion prescription adopted in the EL model. In this regime, the growth of light seeds is inefficient and, therefore, the MBH population originates preferentially from heavy seeds (Trinca et al. 2022). Conversely, in the SE scenario a fraction of the light seed population can grow efficiently already at early times driven by repeated bursts of super-Eddington accretion, resulting in a wider distribution at the low-mass end.

CAT predictions suggest therefore that the overmassive systems detected by JWST are more consistent with a population of objects where the central BHs experienced accelerated growth through repeated episodes of super-Eddington accretion driven by their host galaxy dynamical interactions.

As shown in Figure 1, the SE model predicts a maximum BH-to-stellar mass ratio of  $\sim 0.1$  for the galaxy population at  $4 \lesssim z \lesssim 7$ , reflecting the simultaneous enhancement of star formation and BH accretion rates during major galaxy mergers (see Section 2.4), combined with the assumption that enhanced BH accretion can not be sustained in gas-poor environments, where  $M_{gas}/M_{BH} < 10$  (see Trinca et al. 2022, for details). Therefore, within our SE scenario, the existence of AGNs with extreme  $M_{BH}/M_{star}$  ratios suggests that, while merger-driven gas inflows enhance both BH accretion and star formation, their cumulative impact leads to a rise in the BH-to-stellar mass ratio compared to standard quiescent evolution.

#### 3.1. Properties of overmassive BHs and their hosts

In what follows, we analyse a sample of simulated systems in the SE model that best reproduce the observed AGN population at  $z > 4$ . To do so, we select systems from the SE simulated catalogue at  $z = 5$  and  $z = 6$  with an expected number density large enough to result in at least 1 object in the area covered by the JADES-Medium survey, equal to  $190 \text{ arcmin}^2$ . Additionally, we require the systems to host a nuclear BH significantly more massive than expected from the local scaling with

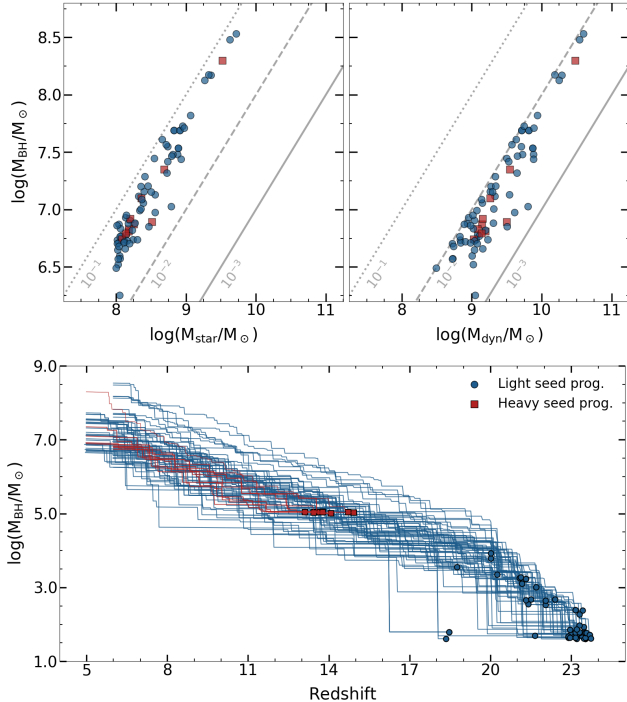


**Figure 2.** Top panels: the CAT synthetic candidates at  $z \sim 5$  and  $z \sim 6$  in the  $M_{\text{BH}} - M_{\text{star}}$  and  $M_{\text{BH}} - M_{\text{dyn}}$  planes. Diagonal lines show constant ratio values of  $10^{-1}$ ,  $10^{-2}$  and  $10^{-3}$ . Bottom panel: the initial seed masses and the subsequent BH evolutionary tracks for the selected systems. BHs originated from light and heavy seeds are represented, respectively, as blue dots and red squares.

the host galaxy’s stellar mass ( $\log(M_{\text{BH}}/M_{\text{star}}) > -2$ ), but closer to the expected relation with the estimated galaxy dynamical mass ( $\log(M_{\text{BH}}/M_{\text{dyn}}) < -2$ ). With this choice, we ensure to focus on a population that resembles more closely the BHs observed by Maiolino et al. (2024b) and Juodžbalis et al. (2024). We do not apply here any selection based on the luminosity of the investigated systems. This would require accounting for several critical factors affecting their observability, including potential obscuration, the impact of highly episodic accretion (see Sec. 3.3), and the detectability of AGN signatures such as broad emission lines. Our primary goal here is instead to investigate the nature and potential evolutionary pathway of the observed population.

The selected sample is shown in the upper panels of Figure 2, where we also indicate if the MBH originates from a light (blue) or a heavy (red) initial seed. Among the total population of 78 systems, only 10 arise from heavy seeds ( $\simeq 13\%$ ). This we believe reflects the lower efficiency of the formation of heavy seed, which requires more restrictive environmental conditions, as described in section 2 (see also Lodato & Natarajan 2007; Valiante et al. 2016; Sassano et al. 2021); this relative proportion

also depends on the adopted prescription for SE growth, which allows light seeds to rapidly increase their mass, making them equally competitive in driving the growth of massive BHs, and their significantly larger number density is reflected in the selected MBH sample shown in Figure 2. The figure shows that the properties of the host galaxies and their nuclear BHs do not depend on the initial seed mass by this epoch in cosmic time. In fact, we find no significant differences between systems descending from light and heavy seeds in the BH-stellar mass and BH-dynamical mass planes. This is also confirmed by the BH evolutionary tracks shown in the bottom panel of the figure. The tracks show that, by the time the first heavy seeds form, in the redshift interval  $z \sim 13 - 15$ , several light seed descendants have been able to grow to masses comparable or even higher than the heavy seed ones (see also Pezzulli et al. 2016), and no peculiar features in the BH evolutionary tracks allow to discern the evolution of the two populations from thereon.

It is worth noting that, while in CAT we find DCBHs formed in pristine atomic cooling halos even at earlier times in a cosmological environment (see for instance Trinca et al. 2022), the high photodissociating background flux required to prevent fragmentation could be provided only in very large overdensities, which are extremely rare at  $z > 15$ . Consequently, these systems would not match the estimated number density of JWST-detected MBHs and are excluded from our sample selection. Assuming a more widespread mechanism of formation for heavy seeds at early times, or a less efficient growth through accretion of lighter BH seeds (Smith et al. 2018) would naturally shift the obtained proportion in favour of the former population.

### 3.2. Decoupled galaxy - BH growth

In this Section we explore the evolution in time of the stellar component in galaxies hosting overmassive BHs. To assess the influence of BH feedback, we discriminate between star formation occurring *in situ*, namely within the same halo of the most massive BH, and *ex situ*, i.e. in other progenitor galaxies of the final system.

Figure 3 shows the average fraction of the galaxy’s final stellar mass that has formed by a given redshift, distinguishing between *in situ* and *ex situ* star formation. The results are presented separately for MBH populations originating from *light* seeds (upper panel) and *heavy* seeds (lower panel). In both panels, the shaded regions represent the  $1\sigma$  dispersion in the star formation histories of galaxies in the selected sample. As shown, the deviation from the average *in situ* evolution is larger at early cosmic epochs, as a consequence of the differ-

ent seed formation times, and becomes smaller at lower redshifts ( $z \lesssim 8$ ). This suggests that the selected overmassive systems share a similar assembly history in the last few hundred Myr of their evolution, even while their early histories were more diverse in terms of both seed mass and growth mode (EL or SE).

We find that at  $z \gtrsim 8$  a significant fraction,  $\sim 30\%$  (on average), of the stellar mass grows in progenitor galaxies which do not co-evolve with the MBH, independently of whether the MBH descends from a light or a heavy seed. At  $z \sim 8$ , the systems enter a distinct evolutionary phase, during which the actual BH-galaxy co-evolution appears to commence. In this later stage, the galaxy assembles the majority of its stellar mass, with most systems building up over 70% of their final  $M_{\text{star}}$ .

These results reflect the efficiency of BH accretion and feedback in the early stages of BH seed growth. At  $z \gtrsim 8$ , the primary BH progenitor evolves rapidly within halos that are undergoing frequent dynamical interactions due to their characteristic hierarchical assembly history in which repeated episodes of SE accretion are triggered, effectively suppressing star formation in their host galaxies.

At  $z < 8$ , the central BH continues to grow efficiently, but its feedback effect on hosts is weaker. This is due to two factors. On the one hand, the occurrence of major merger events - and thus of strong BH-driven feedback phases - decreases at lower redshift (Ferreira et al. 2020), so that the host galaxy star formation becomes more efficient and the stellar mass grows faster. Meanwhile, as the host DM halos grow in mass, deepening their gravitational potential well, the gas outflows are less effective at decreasing the gas content and depleting the gas reservoir.

### 3.3. Duration of Super-Eddington bursts

It is interesting to explore the typical duration and frequency of super-Eddington accretion episodes that overmassive BHs experience during their evolution. This is shown in Figure 4. The distribution of the duration of single SE accretion bursts is presented in the upper panel, which shows that the typical values are very short, and range between 0.5 – 3 Myrs, with a median value of  $\Delta t_{\text{burst}} \simeq 1$  Myr. This is consistent with the typical duration of SE phases suggested by high-resolution hydrodynamical simulations (Sassano et al. e.g. 2023; Massonneau et al. e.g. 2023; Lupi et al. e.g. 2024a; Gordon et al. e.g. 2024, see also the discussion in section 6).

The bottom panel of Figure 4 shows instead the total AGN duty cycle of the selected sample, defined as the fraction of cosmological time spent in a phase SE

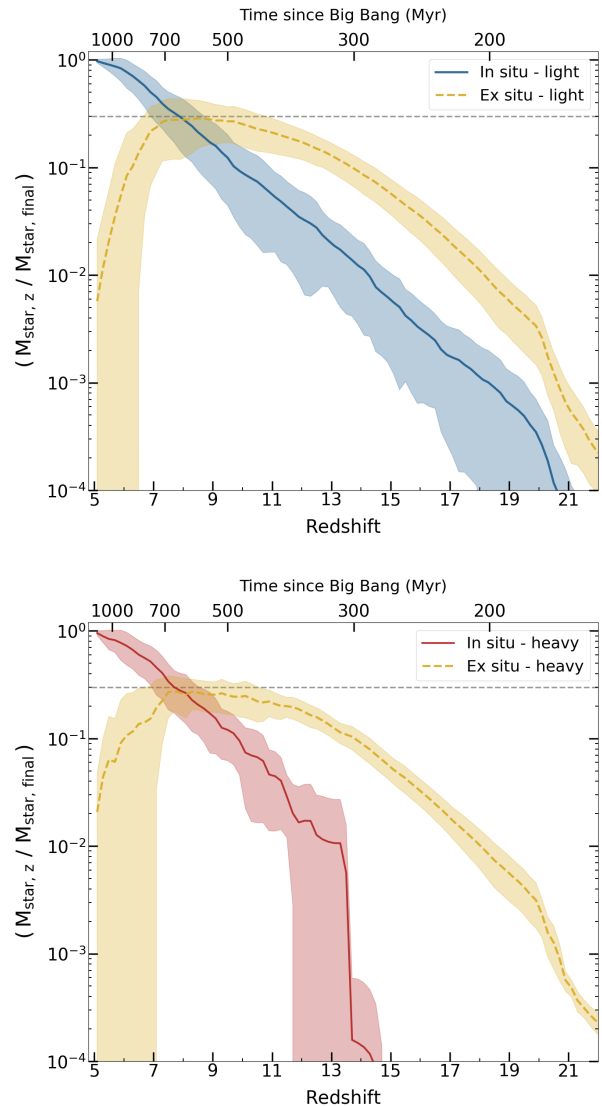


**Figure 3.** Time evolution of the average fraction of the galaxy stellar mass hosting MBHs that descend from light (upper panel) and heavy (lower panel) BH seeds. The solid and dashed lines represent the stellar mass fractions which form *in situ* (i.e. within the same galaxy hosting the final BH) and *ex situ* (i.e. in other galactic progenitors). Shaded regions show the  $1\sigma$  standard deviation from the average evolutionary history. The corresponding cosmological time is reported in the upper axis. The horizontal dashed gray line indicates the 30% of the final galaxy stellar mass.

accretion during repeated episodes of growth. We find SE duty cycles of a few percent, which increase with BH mass ranging from 0.5% for  $M_{\text{BH}} \sim 10^{6.5} M_{\odot}$  to 6% for  $M_{\text{BH}} \sim 10^{8.5} M_{\odot}$ . This relatively small duty cycle implies that in the SE model most of the BHs are largely *dormant* and only a small fraction can be observed in

their active phase (see Juodžbalis et al. 2024). This issue will be discussed further in Section 4.

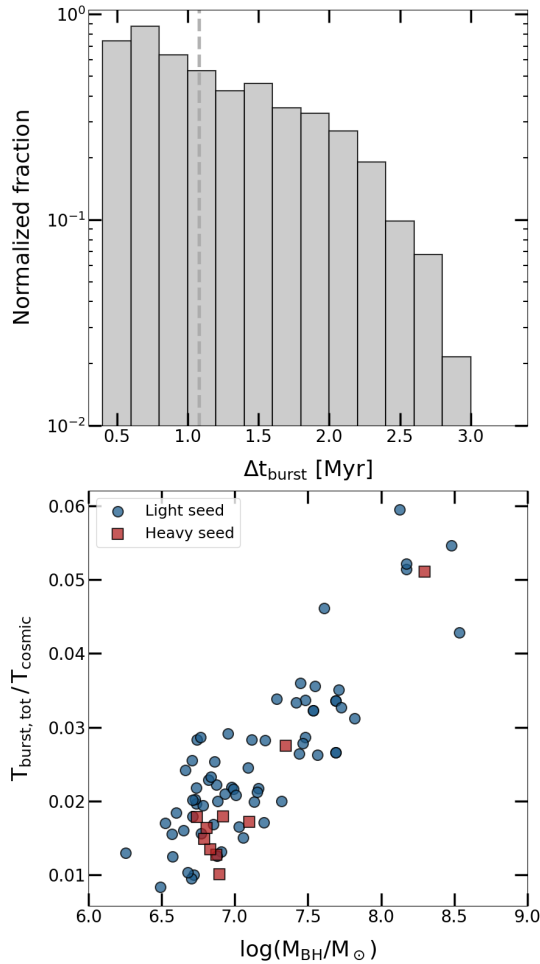


**Figure 4.** *Top panel:* distribution of the time duration of super-Eddington accretion bursts for the selected SMBH population shown in Figure 2. The grey vertical line shows the median of the distribution. *Bottom panel:* total fraction of the cosmological time spent in a burst phase as a function of the final BH mass. The points are color-coded according to the seeding scenario as in Figure 2.

#### 4. MASSIVE DORMANT BLACK HOLES

The evolution of overmassive systems through short phases of super-Eddington accretion leads to short AGN duty cycles, of the order of few percent. This implies that a large fraction of the MBH population is largely “dormant”, i.e. accreting significantly below the Eddington limit, with  $\lambda_{\text{Edd}} = L_{\text{bol}} / L_{\text{Edd}} \lesssim 0.05$  (Schneider et al. 2023). This scenario poses substantial challenges for the detection of these early accreting BHs, since only galaxies hosting the most massive ones would exhibit

clear signatures of the nuclear source, such as a broad emission line component.

Recently, Juodžbalis et al. (2024) reported the detection of an overmassive dormant BH hosted in the JADES GN-1001830 galaxy at  $z = 6.67$ . The system has been covered with NIRCcam and NIRSPEC observations, revealing clear broad  $H\alpha$  emission with a Full Width at Half Maximum (FWHM) of  $\sim 5700 \text{ km s}^{-1}$ , which leads to an estimated BH mass of  $\log(M_{\text{BH}} / M_{\odot}) = 8.61^{+0.27}_{-0.24}$ . The broad component appears to be symmetrical, and no broad emission is observed in [OIII], disfavouring the possibility of it being associated with an outflow. The AGN bolometric luminosity,  $L_{\text{bol}} \sim 3 \times 10^{43} \text{ ergs}^{-1}$ , estimated from the broad  $H\alpha$  component using the scaling relation by Stern & Laor (2012), implies an Eddington ratio  $\lambda_{\text{Edd}} = 0.024^{+0.011}_{-0.008}$ . Finally, a stellar mass of  $\log(M_{*} / M_{\odot}) = 8.92^{+0.30}_{-0.31}$  and a star formation rate of  $\text{SFR} = 1.38^{+0.92}_{-0.45} M_{\odot} \text{ yr}^{-1}$  have been inferred from the SED fitting of the 8 photometric bands using the fitting codes BAGPIPES (Carnall et al. 2018) and Prospector (Johnson et al. 2021). The dormant nature of this black hole allows for a more reliable study of its host galaxy compared to the highly accreting counterparts in the bright quasar phase, where the nuclear emission overshines the galaxy. The MBH residing in GN-1001830 is suggested to be significantly overmassive with respect to the host galaxy, with a mass ratio  $M_{\text{BH}} / M_{*} \sim 0.4$ , almost 3 dex above what is expected from the local scaling relation (Reines & Volonteri 2015). As shown by Juodžbalis et al. (2024), the properties of GN-1001830 are well explained by the CAT SE model, which predicts this system to be the tip of the iceberg of a vast population of dormant BHs at a similar redshift range (for more details see Figure 3 of Juodžbalis et al. 2024, and the thorough discussion therein).

As a follow-up of that analysis, here we investigate the evolutionary tracks of simulated systems in the SE model whose properties - namely the BH mass, stellar mass and SFR - are consistent with that of GN-1001830 observed at  $z = 6.67$  within the uncertainties on the estimated values. For the selected systems, we trace back in time the evolution of the host galaxy and its progenitors. In Figure 5 we compare the predictions of the Prospector and BAGPIPES SED fitting models for GN-1001830 with the SF histories (SFHs) predicted by CAT smoothed over a timescale of approximately 50 Myr to eliminate short-term variability, which is not resolved by SED fitting models. The SED fitting has been performed assuming the stellar component dominates the source emission, but excluding filter bands associated with strong AGN emission lines which might contaminate the analysis. In CAT galaxies the rate of



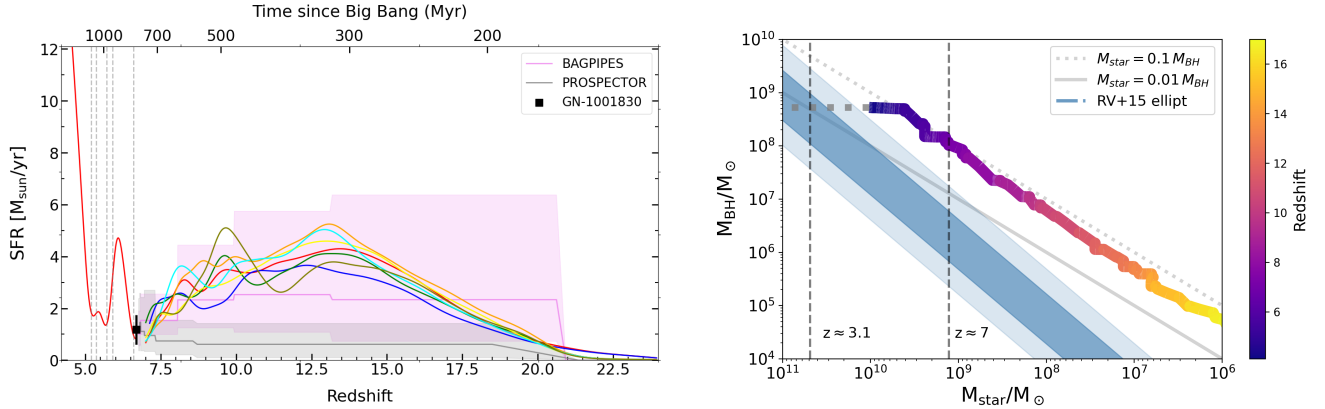


**Figure 5.** *Left panel:* Star formation history of the best synthetic counterparts of JADES GN-1001830 at  $z \sim 7$  (see text). Evolutionary tracks are compared to the SFH predicted by Prospector (grey shaded area) and Bagpipes (pink shaded area) from the host galaxy SED fitting (Juodžbalis et al. 2024). For one of the candidates, we show the SFR evolution down to  $z = 4$ . Vertical dashed lines mark the occurrence of major mergers involving the AGN host galaxy. *Right panel:* Evolution in redshift of the  $M_{\text{BH}}/M_{\text{star}}$  ratio for the selected counterpart of GN-1001830 (red line in the left panel). Dark and light blue shaded areas mark the region consistent with the local scaling relation from Reines & Volonteri (2015) within  $1\sigma$  and  $2\sigma$ , respectively. The vertical line shows the cosmic epoch when the system is expected to enter the local scaling, assuming the central MBH remains dormant.

star formation slowly increases with time down to redshift  $z \sim 10 - 12$ , below which it decreases, reaching the value inferred from the observations of GN-1001830 (black squared data point). Overall, the SFHs predicted by CAT are consistent with that inferred using BAGPIPES, within the uncertainties of that model (pink shaded region), supporting a relatively flat SFH, with the SFR remaining constant, within a factor of 3, in the redshift range  $z \sim 7 - 17$ . In the same figure, the solid red line shows the SFH of one of the systems predicted by CAT down to  $z \simeq 4$  (the final redshift of our simulation). The vertical dashed lines indicate the redshift at which this system experiences major mergers, which - in the SE model - trigger SE BH accretion. The star formation rate rapidly increases between major merger events, when BH accretion and feedback becomes less efficient. In this system, the last major merger event occurs at  $z \sim 5.18$  and the SFR continuously increases thereafter becoming one order of magnitude higher by  $z = 4$ . As a result, the stellar component grows faster than the MBH, doubling its mass and reaching a value  $\log(M_*/M_\odot) \simeq 10.0$  in  $\Delta t \sim 300\text{Myr}$ . At  $z \simeq 4$ , the BH-to-stellar mass ratio is  $\sim 0.05$ .

The evolution in redshift of the  $M_{\text{BH}}/M_{\text{star}}$  ratio for the selected evolutionary track is shown in Figure 5. It is clear how the system evolves along the  $M_{\text{BH}}/M_{\text{star}} \sim 0.1$  relation down to  $z \approx 7$ , when the occurrence of prolonged phases where the central BH remains 'dormant' drive the system toward lower mass ratios. Given this result, it is interesting to provide a simple analytical estimate of the time required for the galaxy to arrive at the local  $M_{\text{BH}} - M_{\text{star}}$  scaling relation. To this aim

we assume that the galaxy does not undergo significant dynamical interactions during its subsequent evolution, so that the nuclear BH remains dormant. Considering a redshift evolution of the galaxy specific SFR as  $s\text{SFR} = \text{SFR}/M_{\text{star}} \propto (1+z)^{1.6}$  (see Di Cesare et al. 2023), we estimate that the system shown by the red line in Figure 5 would need  $\sim 0.50$  Gyr ( $z \sim 3.1$ ) to lie within  $1\sigma$  from the local scaling relation by Reines & Volonteri (2015) for elliptical galaxies. This is illustrated in the right panel of Fig. 5. Notably, the  $M_{\text{BH}} - M_{\text{star}}$  relation for elliptical galaxies in the local Universe is steeper than what is observed for AGNs. This implies higher expected  $M_{\text{BH}}/M_{\text{star}}$  ratios in massive galaxies, offering additional support for the hypothesis that these systems could align with local observations through moderate evolution of the black hole-to-stellar mass ratio.

## 5. THE AGN LUMINOSITY FUNCTION AT $5 < z < 7$

In Trinca et al. (2022) we found that merger-driven SE accretion results in a higher number density of bright sources compared to the Eddington-limited scenario, especially in the range  $L_{\text{bol}} \simeq 10^{45} - 10^{47}$  erg/s. It is interesting to revisit this finding in light of the large number density of AGNs identified by JWST, both as type-I/type-II AGNs (see e.g. Harikane et al. 2023; Maiolino et al. 2024b; Scholtz et al. 2023) and as LRDs (see e.g. Matthee et al. 2024; Greene et al. 2024; Kokorev et al. 2023; Akins et al. 2024). These studies show that the number density of JWST-detected systems lies between 1 to 2 dex larger than the extrapolation of the luminosity function probed by the optically and UV selected quasar

population at  $z \simeq 5 - 6$  (Niida et al. 2020; Shen et al. 2020), and higher than the estimated density from the deep X-ray observations (Giallongo et al. 2015, 2019).

In Figure 6 we show the AGN bolometric luminosity function (LF) predicted by CAT in the redshift range  $5 < z < 7$  (black squares) for the Eddington-limited and super-Eddington models (upper and lower panel, respectively). Notably, the AGN bolometric LF predicted by the SE model at  $L_{\text{bol}} = (10^{45} - 10^{47}) \text{ erg s}^{-1}$  is in good agreement with that derived for the LRD population by Akins et al. (2024, red circles)<sup>1</sup>. In the SE model, the predicted rise of the luminosity function above  $L_{\text{bol}} > 10^{45} \text{ erg/s}$  results from the population of smaller-mass black holes undergoing brief episodes of SE growth, which leads to a marked boost in their luminosity. Due to the steep BH mass function, even a small fraction of active lower-mass black holes can provide a substantial contribution to the bright end of the distribution, in contrast to more massive systems undergoing a steady, sub-Eddington growth phase.

In both the EL and SE scenarios the predicted bolometric LF drops by more than two orders of magnitude below the number density estimated by Akins et al. (2024) at the bright-end of the distribution, for  $L_{\text{bol}} \gtrsim 10^{46.5} \text{ erg/s}$ . It is worth mentioning, though, that their estimated bolometric LF relies on the assumption that the AGNs dominate the SEDs. Several studies suggest that both the stellar and the AGN components contribute to the SED (see e.g. Volonteri et al. 2024; Taylor et al. 2024), especially in the UV band, thus resulting in a lower estimated AGN luminosity, that would be more consistent with the results of mid-IR and X-ray surveys (Williams et al. 2023; Pérez-González et al. 2024; Yue et al. 2024a; Ananna et al. 2024), and still in agreement with CAT predictions. This agreement suggests that the population of LRDs might represent a transient phase in early galaxy evolution, during which the emission is AGN-dominated due to a brief period of enhanced BH accretion, possibly triggered by major galaxy merger or other relevant dynamical interactions.

## 6. DISCUSSION

The comparison between the overmassive BH population observed at  $z > 4$  and the prediction of CAT models suggests that early BH growth could be dominated by short, repeated bursts of super-Eddington accretion. Interestingly, in our SE model, less than 15% of the whole

<sup>1</sup> These authors analysed more than 400 LRDs detected in the COSMOS-Web survey (Casey et al. 2023) at  $z > 4$ , and recover the bolometric luminosity from the intrinsic SED modelling, assuming that the overall emission is AGN dominated.

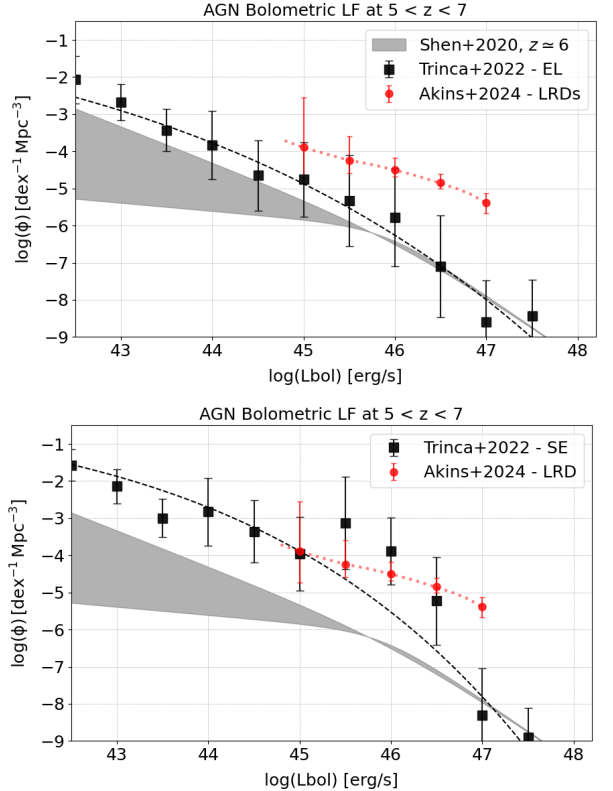


**Figure 6.** AGN bolometric luminosity function at  $5 < z < 7$ . CAT predictions for the Eddington-limited (upper panel) and super-Eddington (lower panel) scenarios are shown as black squares, and are compared with the recent estimate of the bolometric luminosity function derived for the *Little Red Dots* by Akins et al. (2024) (red circles). We also report in grey the quasar bolometric LF at  $z \approx 6$  derived from UV-selected quasars in Shen et al. (2020).

population of overmassive BHs at these epochs descends from heavy seeds thus their detection is not necessarily an indication of the existence of heavy seeds (however this is not the case for earlier cosmic epochs, like  $z \sim 10$ , see for instance Natarajan et al. 2024). In addition, we find that the typical AGN duty cycle of CAT SE systems is  $\sim 1 - 6\%$ , independent of the initial seed mass. Such short duty cycles are supported by recent clustering analysis of quasars and galaxies observed with JWST at  $z \sim 6$  (Pizzati et al. 2024; Eilers et al. 2024). In our model, SE accretion is triggered during major galaxy mergers and sustained for brief periods of time (a few million years). Although our description of BH accretion and feedback in the super-Eddington regime is highly simplified (see Section 2.4), the predicted duration of SE accretion bursts are consistent with those estimated by high-resolution hydrodynamical simulations of isolated gas rich galaxies hosting BHs of  $10^3 - 10^4 M_{\odot}$  (e.g. Lupi et al. 2016; Sassano et al. 2023; Massonneau

et al. 2023; Gordon et al. 2024; Lupi et al. 2024a; Shi et al. 2024). In these dense environments, the interaction with dense gas clumps likely enables super/hyper-Eddington accretion that is sustained for a few BHs, for up to a few tens of million years, depending on the mechanical/kinetic feedback efficiency. Observations from JWST suggest that early galaxies are gas-rich and characterized by extremely dense and compact clumps (Fujimoto et al. 2024), providing favourable conditions for super-Eddington growth (Guia et al. 2024). It has to be noted that, although major galaxy mergers have been suggested as a possible mechanism to contrast the negative effect of mechanical feedback onto BH growth and promote efficient accretion, their role in directly triggering/enhancing BH growth is still poorly explored with simulations. A shorter duration of accretion bursts onto the BH, possibly regulated by strong AGN feedback, might limit the growth of lighter BH seeds compared to our findings (Regan et al. 2019). The nature of these short bursts of super-Eddington accretion and their interplay with the star formation process across different galaxy and BH mass scales will be the subject of a detailed study through high-resolution isolated simulations in Zana et al. (in prep), which will provide valuable insights to refine the predictions of semi-analytical models.

An early massive BH whose growth is dominated by short-repeated phases of super-Eddington accretion has several implications for the observable features of these systems. As shown in Section 5, it could help explain the large observed number density of AGNs, particularly among the LRD population, wherein it may represent a transient phase in early black hole evolution. Interestingly, with few exceptions (Kocevski et al. 2023; Bogdán et al. 2024; Kovács et al. 2024), the AGNs detected by JWST are not detected in X-rays (Maiolino et al. 2024c; Ananna et al. 2024), and none have been found in radio observations to date (Mazzolari et al. 2024b). Several explanations have been proposed, including strong AGN obscuration, differential obscuration, or intrinsically X-ray weak AGN spectra (Maiolino et al. 2024c; Ananna et al. 2024; Inayoshi & Maiolino 2024) for these sources. Regimes of super-Eddington BH accretion are expected to be characterized by the formation of a geometrically and optically thick accretion disk, resulting in strong collimated emission. Recent studies propose that this altered accretion geometry could lead to softer X-ray spectra, characterized by a steeper photon index and a lower-energy cutoff. This effect is potentially caused by the overcooling of the coronal plasma embedded in a funnel-like structure (Madau & Haardt 2024), along with the low likelihood of observing strongly beamed X-ray emission aligned with the jet (Pacucci & Narayan

2024; King 2024). Notably, analogous spectral features have been observed in different AGN surveys, targeting both the population of more luminous and massive quasars detected at  $z \gtrsim 7$  (Zappacosta et al. 2020, 2023) and samples of more local supermassive BHs accreting at super-Eddington rates (Tortosa et al. 2023). However, the full multi-wavelength signatures of SE accretion remain currently unsettled. Although a handful of sources with implicated SE accretion have been identified in the redshift range explored in this work, there is considerable variation in their detected rest-frame UV-optical and X-ray fluxes. For instance, the source LID-568 ( $z = 4.4$ , Suh et al. 2024) appears X-ray bright, while other systems, like PSO J006+39 ( $z = 6.6$ , Tang et al. 2019), exhibit signatures of highly obscured, geometrically thick accretion disks.

Meanwhile, high Eddington ratios could also mitigate the tension between the observed overmassive AGNs detected by JWST and the local relation. Indeed, Lupi et al. (2024b) showed that, as a consequence of the modified disk geometry, for high Eddington ratios the self-shadowing effect of the accretion disk may lead to overestimating the BH masses by up to an order of magnitude when relying on the standard, single-epoch virial methods, based on local reverberation mapping calibrations. Recent direct, interferometric measurement of the BLR in a distant quasar accreting highly super-Eddington revealed an offset ranging between 0.43–0.73 dex, depending on the chosen calibrator (Abuter et al. 2024).

An additional concern has been raised by Inayoshi & Ichikawa (2024). They show that, under the assumption of an AGN-dominated emission and a population spanning the wide redshift range where LRDs are detected ( $4 \lesssim z \lesssim 8$ , Kocevski et al. 2024), the BH mass density accreted by LRDs at  $z > 4$  would already exceed the local BH mass density. While they invoke the need for high radiative efficiencies during early BH accretion, suggesting higher BH spin, this tension might be similarly alleviated assuming a growth history marked by very short-lived phases of efficient BH accretion — significantly shorter than the observational time window covered by the LRD sample, of the order of  $\sim 1$  Myr as we report here.

Interestingly, Mezcua et al. (2024) recently reported the detection of 12 overmassive BHs in low-mass galaxies observed at cosmic noon ( $z \sim 1 - 3$ ) in the VIMOS Public Extragalactic Redshift Survey (VIPERS) (shown in Figure 1). These galaxies present physical properties - such as BH mass, stellar mass, bolometric luminosity, Eddington ratio - that are remarkably similar to the ones inferred for the high- $z$  AGNs observed by JWST, suggesting that we might be observing systems in an

analogous phase of their evolution, but during different cosmic epochs. If we assume that galaxies hosting overmassive BHs transit to the local scaling relations on timescales comparable to those estimated by CAT ( $\sim 0.5$  Gyrs), this could explain why systems with such extreme  $M_{\text{BH}}/M_{\text{star}}$  ratios may not have been observed at  $z \simeq 0$ .

## 7. CONCLUSIONS

In this study, we show that properties of AGNs observed by JWST at  $5 < z < 7$  can be explained in a scenario where light and heavy BH seeds grow through short phases of super-Eddington accretion. In our Cosmic Archaeology Tool semi-analytical model, these phases are triggered by galaxy major mergers. We reconstruct the evolutionary pathways of overmassive BHs at  $5 < z < 7$ , investigating how these BHs accumulate mass over cosmic time and interact with their host galaxies.

We find that:

- Overmassive BHs with properties consistent with JWST observations can originate from both light and heavy seeds. In particular, the vast majority ( $> 85\%$ ) of systems predicted by CAT showing analogous properties descends from light-PopIII remnant seeds formed at  $z > 20$ , while only a minority originates from a direct collapse BH formed between  $z \sim 13 - 15$ . The highly efficient episodes of accretion cause the information on the nature of the BH seed to be rapidly erased, making it difficult to differentiate between these formation pathways for individual sources by  $z \sim 8$ .
- The selected galaxy population shows a common characteristic evolutionary history, independent of the BH seeding channel. At  $z > 8$ , the stellar component and the main MBH progenitor face a decoupled evolution, i.e., they grow in different halos. The MBH-galaxy co-evolution starts only at  $z \sim 8$ , when the galaxy has assembled, on average, 30% of its final stellar mass. In the subsequent evolutionary phase, the impact of MBH feedback on the galaxy decreases in importance as a result of the decreasing number of super-Eddington events and the growth of the halo’s gravitational potential.
- Our model predicts relatively short evolutionary timescales and duty cycles associated with the formation of overmassive systems, even when starting from smaller BH seeds. We find that single episodes of super-Eddington accretion typically last between  $0.5 - 3$  Myr, with a median value of  $\sim 1$  Myr, resulting in a total AGN duty cycle of

$\sim 1 - 4\%$ . No clear correlation is observed between the growth timescale and the nature of the initial seed, confirming that BH growth is primarily governed by their evolutionary environment. These short duty cycles suggest that a large fraction of the MBH population at high redshift is in an inactive phase, as supported by current observations, including the dormant overmassive BH detected in the JADES GN-1001830 galaxy at  $z \sim 6.67$ .

- Tracking the evolution down to  $z = 4$  of CAT systems matching the properties of JADES GN-1001830, we find that, as the frequency of major mergers decreases, the BH growth slows down, allowing for the rapid build-up of the stellar component. In the absence of strong dynamical interactions that could re-activate efficient bursts of super-Eddington accretion on the nuclear BH, the star formation rate can quickly rise, increasing the galaxy stellar mass by  $\sim 1$  dex by  $z = 4$  as seen in some of the selected systems. This transition drives these galaxies toward lower BH-to-stellar mass ratios, allowing them to fall in line with the local scaling relations in approximately  $\sim 0.5$  Gyrs, assuming the MBH remains dormant during this entire interval.
- The enhancement in BH luminosity associated with short periods of super-Eddington accretion results in an AGN luminosity function at  $5 < z < 7$  well aligned with recent JWST observations. Specifically, the CAT super-Eddington model closely reproduces the high number density of accreting BHs with  $L_{\text{bol}} = 10^{45} - 10^{47}$  erg/s, as inferred from the population of “Little Red Dots”, under the assumption that their emission is primarily AGN-dominated. This consistency supports the idea that this population might represent a transient phase in early galaxy evolution.

## ACKNOWLEDGMENTS

AT sincerely thanks the Kavli Institute for Cosmology, Cambridge (KICC) for their extended hospitality that greatly influenced and supported the development of this work. This research was supported in part by grant NSF PHY-2309135 to the Kavli Institute for Theoretical Physics (KITP). AT, RS and RV thanks the KITP and the organisers of the “Cosmic Origins: The First Billion Years” program for useful discussions and their hospitality during the program, which significantly contributed to the development of this work. AT, RV, and AL acknowledge support from PRIN MUR “2022935STW”. AT, RS and RV acknowledge finan-

cial support from the Bando Ricerca Fondamentale INAF 2023, Theory Grant “Theoretical models for Black Holes Archaeology” and Mini-grant “Cosmic Archaeology with the first black hole seeds”. RV acknowledge financial support from the Bando Ricerca Fondamentale INAF 2022 Large Grant “Toward an holistic view of the Titans: multi-band observations of  $z > 6$  QSOs powered by greedy supermassive black-holes”. RS, LG, and TZ acknowledge support from the PRIN 2022 MUR project 2022CB3PJ3—First Light And Galaxy aSsembly (FLAGS) funded by the European Union—Next Generation EU, and from EU-Recovery Fund PNRR - National Centre for HPC, Big Data and Quantum Computing. LG acknowledges support from the Amaldi Re-

search Center funded by the MIUR program “Dipartimento di Eccellenza” (CUP:B81I18001170001). PN acknowledges support from the Gordon and Betty Moore Foundation and the John Templeton Foundation that fund the Black Hole Initiative (BHI) at Harvard University where she serves as an external PI. RM acknowledges support by the Science and Technology Facilities Council (STFC), by the ERC through Advanced Grant 695671 ”QUENCH”, and by the UKRI Frontier Research grant RISEandFALL. RM also acknowledges funding from a research professorship from the Royal Society.

## REFERENCES

- Abuter, R., Allouche, F., Amorim, A., et al. 2024, *Nature*, 627, 281, doi: [10.1038/s41586-024-07053-4](https://doi.org/10.1038/s41586-024-07053-4)
- Akins, H. B., Casey, C. M., Lambrides, E., et al. 2024, arXiv e-prints, arXiv:2406.10341, doi: [10.48550/arXiv.2406.10341](https://doi.org/10.48550/arXiv.2406.10341)
- Ananna, T. T., Bogdán, Á., Kovács, O. E., Natarajan, P., & Hickox, R. C. 2024, *ApJL*, 969, L18, doi: [10.3847/2041-8213/ad5669](https://doi.org/10.3847/2041-8213/ad5669)
- Baggen, J. F. W., van Dokkum, P., Brammer, G., et al. 2024, *ApJL*, 977, L13, doi: [10.3847/2041-8213/ad90b8](https://doi.org/10.3847/2041-8213/ad90b8)
- Barro, G., Perez-Gonzalez, P. G., Kocevski, D. D., et al. 2023, arXiv e-prints, arXiv:2305.14418, doi: [10.48550/arXiv.2305.14418](https://doi.org/10.48550/arXiv.2305.14418)
- Barro, G., Pérez-González, P. G., Kocevski, D. D., et al. 2024, *ApJ*, 963, 128, doi: [10.3847/1538-4357/ad167e](https://doi.org/10.3847/1538-4357/ad167e)
- Bogdán, Á., Goulding, A. D., Natarajan, P., et al. 2024, *Nature Astronomy*, 8, 126, doi: [10.1038/s41550-023-02111-9](https://doi.org/10.1038/s41550-023-02111-9)
- Bondi, H. 1952, *MNRAS*, 112, 195, doi: [10.1093/mnras/112.2.195](https://doi.org/10.1093/mnras/112.2.195)
- Carnall, A. C., McLure, R. J., Dunlop, J. S., & Davé, R. 2018, *MNRAS*, 480, 4379, doi: [10.1093/mnras/sty2169](https://doi.org/10.1093/mnras/sty2169)
- Casey, C. M., Kartaltepe, J. S., Drakos, N. E., et al. 2023, *ApJ*, 954, 31, doi: [10.3847/1538-4357/acc2bc](https://doi.org/10.3847/1538-4357/acc2bc)
- Chisholm, J., Berg, D. A., Endsley, R., et al. 2024, *MNRAS*, 534, 2633, doi: [10.1093/mnras/stae2199](https://doi.org/10.1093/mnras/stae2199)
- de Bennassuti, M., Salvadori, S., Schneider, R., Valiante, R., & Omukai, K. 2017, *MNRAS*, 465, 926, doi: [10.1093/mnras/stw2687](https://doi.org/10.1093/mnras/stw2687)
- de Bennassuti, M., Schneider, R., Valiante, R., & Salvadori, S. 2014, *MNRAS*, 445, 3039, doi: [10.1093/mnras/stu1962](https://doi.org/10.1093/mnras/stu1962)
- Di Cesare, C., Graziani, L., Schneider, R., et al. 2023, *MNRAS*, 519, 4632, doi: [10.1093/mnras/stac3702](https://doi.org/10.1093/mnras/stac3702)
- Eilers, A.-C., Mackenzie, R., Pizzati, E., et al. 2024, *ApJ*, 974, 275, doi: [10.3847/1538-4357/ad778b](https://doi.org/10.3847/1538-4357/ad778b)
- Ferreira, L., Conselice, C. J., Duncan, K., et al. 2020, *ApJ*, 895, 115, doi: [10.3847/1538-4357/ab8f9b](https://doi.org/10.3847/1538-4357/ab8f9b)
- Fujimoto, S., Brammer, G. B., Watson, D., et al. 2022, *Nature*, 604, 261, doi: [10.1038/s41586-022-04454-1](https://doi.org/10.1038/s41586-022-04454-1)
- Fujimoto, S., Ouchi, M., Kohno, K., et al. 2024, arXiv e-prints, arXiv:2402.18543, doi: [10.48550/arXiv.2402.18543](https://doi.org/10.48550/arXiv.2402.18543)
- Furtak, L. J., Zitrin, A., Plat, A., et al. 2023, *ApJ*, 952, 142, doi: [10.3847/1538-4357/acdc9d](https://doi.org/10.3847/1538-4357/acdc9d)
- Furtak, L. J., Labbé, I., Zitrin, A., et al. 2024, *Nature*, 628, 57, doi: [10.1038/s41586-024-07184-8](https://doi.org/10.1038/s41586-024-07184-8)
- Giallongo, E., Grazian, A., Fiore, F., et al. 2015, *A&A*, 578, A83, doi: [10.1051/0004-6361/201425334](https://doi.org/10.1051/0004-6361/201425334)
- . 2019, *ApJ*, 884, 19, doi: [10.3847/1538-4357/ab39e1](https://doi.org/10.3847/1538-4357/ab39e1)
- Gordon, S. T., Smith, B. D., Khochfar, S., & Beckmann, R. S. 2024, arXiv e-prints, arXiv:2412.06888, doi: [10.48550/arXiv.2412.06888](https://doi.org/10.48550/arXiv.2412.06888)
- Greene, J. E., Labbe, I., Goulding, A. D., et al. 2024, *ApJ*, 964, 39, doi: [10.3847/1538-4357/ad1e5f](https://doi.org/10.3847/1538-4357/ad1e5f)
- Guia, C. A., Pacucci, F., & Kocevski, D. D. 2024, *Research Notes of the American Astronomical Society*, 8, 207, doi: [10.3847/2515-5172/ad7262](https://doi.org/10.3847/2515-5172/ad7262)
- Hainline, K. N., Maiolino, R., Juodzbalis, I., et al. 2024, arXiv e-prints, arXiv:2410.00100, doi: [10.48550/arXiv.2410.00100](https://doi.org/10.48550/arXiv.2410.00100)
- Harikane, Y., Zhang, Y., Nakajima, K., et al. 2023, arXiv e-prints, arXiv:2303.11946, doi: [10.48550/arXiv.2303.11946](https://doi.org/10.48550/arXiv.2303.11946)
- Heger, A., & Woosley, S. E. 2002, *ApJ*, 567, 532, doi: [10.1086/338487](https://doi.org/10.1086/338487)
- Hoyle, F., & Lyttleton, R. A. 1941, *MNRAS*, 101, 227, doi: [10.1093/mnras/101.4.227](https://doi.org/10.1093/mnras/101.4.227)

- Inayoshi, K., & Ichikawa, K. 2024, arXiv e-prints, arXiv:2402.14706, doi: [10.48550/arXiv.2402.14706](https://doi.org/10.48550/arXiv.2402.14706)
- Inayoshi, K., & Maiolino, R. 2024, arXiv e-prints, arXiv:2409.07805, doi: [10.48550/arXiv.2409.07805](https://doi.org/10.48550/arXiv.2409.07805)
- Inayoshi, K., Visbal, E., & Haiman, Z. 2020, *ARA&A*, 58, 27, doi: [10.1146/annurev-astro-120419-014455](https://doi.org/10.1146/annurev-astro-120419-014455)
- Johnson, B. D., Leja, J., Conroy, C., & Speagle, J. S. 2021, *ApJS*, 254, 22, doi: [10.3847/1538-4365/abef67](https://doi.org/10.3847/1538-4365/abef67)
- Juodžbalis, I., Maiolino, R., Baker, W. M., et al. 2024, arXiv e-prints, arXiv:2403.03872, doi: [10.48550/arXiv.2403.03872](https://doi.org/10.48550/arXiv.2403.03872)
- King, A. 2024, *MNRAS*, 531, 550, doi: [10.1093/mnras/stae1171](https://doi.org/10.1093/mnras/stae1171)
- Kocevski, D. D., Onoue, M., Inayoshi, K., et al. 2023, arXiv e-prints, arXiv:2302.00012, doi: [10.48550/arXiv.2302.00012](https://doi.org/10.48550/arXiv.2302.00012)
- Kocevski, D. D., Finkelstein, S. L., Barro, G., et al. 2024, arXiv e-prints, arXiv:2404.03576, doi: [10.48550/arXiv.2404.03576](https://doi.org/10.48550/arXiv.2404.03576)
- Kokorev, V., Fujimoto, S., Labbe, I., et al. 2023, *ApJL*, 957, L7, doi: [10.3847/2041-8213/ad037a](https://doi.org/10.3847/2041-8213/ad037a)
- Kormendy, J., & Ho, L. C. 2013, *ARA&A*, 51, 511, doi: [10.1146/annurev-astro-082708-101811](https://doi.org/10.1146/annurev-astro-082708-101811)
- Kovács, O. E., Bogdán, Á., Natarajan, P., et al. 2024, *ApJL*, 965, L21, doi: [10.3847/2041-8213/ad391f](https://doi.org/10.3847/2041-8213/ad391f)
- Labbe, I., Greene, J. E., Bezanson, R., et al. 2023, arXiv e-prints, arXiv:2306.07320, doi: [10.48550/arXiv.2306.07320](https://doi.org/10.48550/arXiv.2306.07320)
- Larson, R. B. 1998, *Monthly Notices of the Royal Astronomical Society*, 301, 569
- Larson, R. L., Finkelstein, S. L., Kocevski, D. D., et al. 2023, arXiv e-prints, arXiv:2303.08918, doi: [10.48550/arXiv.2303.08918](https://doi.org/10.48550/arXiv.2303.08918)
- Lauer, T. R., Tremaine, S., Richstone, D., & Faber, S. M. 2007, *ApJ*, 670, 249, doi: [10.1086/522083](https://doi.org/10.1086/522083)
- Leung, G. C. K., Bagley, M. B., Finkelstein, S. L., et al. 2023, *ApJL*, 954, L46, doi: [10.3847/2041-8213/acf365](https://doi.org/10.3847/2041-8213/acf365)
- Li, Z., Inayoshi, K., Chen, K., Ichikawa, K., & Ho, L. C. 2024, arXiv e-prints, arXiv:2407.10760, doi: [10.48550/arXiv.2407.10760](https://doi.org/10.48550/arXiv.2407.10760)
- Lodato, G., & Natarajan, P. 2007, *MNRAS*, 377, L64, doi: [10.1111/j.1745-3933.2007.00304.x](https://doi.org/10.1111/j.1745-3933.2007.00304.x)
- Lupi, A., Haardt, F., Dotti, M., et al. 2016, *MNRAS*, 456, 2993, doi: [10.1093/mnras/stv2877](https://doi.org/10.1093/mnras/stv2877)
- Lupi, A., Quadri, G., Volonteri, M., Colpi, M., & Regan, J. A. 2024a, *A&A*, 686, A256, doi: [10.1051/0004-6361/202348788](https://doi.org/10.1051/0004-6361/202348788)
- Lupi, A., Trinca, A., Volonteri, M., Dotti, M., & Mazzucchelli, C. 2024b, arXiv e-prints, arXiv:2406.17847, doi: [10.48550/arXiv.2406.17847](https://doi.org/10.48550/arXiv.2406.17847)
- Madau, P., & Haardt, F. 2024, arXiv e-prints, arXiv:2410.00417, doi: [10.48550/arXiv.2410.00417](https://doi.org/10.48550/arXiv.2410.00417)
- Madau, P., Haardt, F., & Dotti, M. 2014, *ApJL*, 784, L38, doi: [10.1088/2041-8205/784/2/L38](https://doi.org/10.1088/2041-8205/784/2/L38)
- Maiolino, R., Scholtz, J., Witstok, J., et al. 2024a, *Nature*, 627, 59, doi: [10.1038/s41586-024-07052-5](https://doi.org/10.1038/s41586-024-07052-5)
- Maiolino, R., Scholtz, J., Curtis-Lake, E., et al. 2024b, *A&A*, 691, A145, doi: [10.1051/0004-6361/202347640](https://doi.org/10.1051/0004-6361/202347640)
- Maiolino, R., Risaliti, G., Signorini, M., et al. 2024c, arXiv e-prints, arXiv:2405.00504, doi: [10.48550/arXiv.2405.00504](https://doi.org/10.48550/arXiv.2405.00504)
- Massonneau, W., Dubois, Y., Volonteri, M., & Beckmann, R. S. 2023, *A&A*, 669, A143, doi: [10.1051/0004-6361/202244874](https://doi.org/10.1051/0004-6361/202244874)
- Matthee, J., Naidu, R. P., Brammer, G., et al. 2024, *ApJ*, 963, 129, doi: [10.3847/1538-4357/ad2345](https://doi.org/10.3847/1538-4357/ad2345)
- Mazzolari, G., Scholtz, J., Maiolino, R., et al. 2024a, arXiv e-prints, arXiv:2408.15615, doi: [10.48550/arXiv.2408.15615](https://doi.org/10.48550/arXiv.2408.15615)
- Mazzolari, G., Gilli, R., Maiolino, R., et al. 2024b, arXiv e-prints, arXiv:2412.04224, doi: [10.48550/arXiv.2412.04224](https://doi.org/10.48550/arXiv.2412.04224)
- Mezcua, M., Pacucci, F., Suh, H., Siudek, M., & Natarajan, P. 2024, *ApJL*, 966, L30, doi: [10.3847/2041-8213/ad3c2a](https://doi.org/10.3847/2041-8213/ad3c2a)
- Natarajan, P., Pacucci, F., Ferrara, A., et al. 2017, *The Astrophysical Journal*, 838, 117
- Natarajan, P., Pacucci, F., Ricarte, A., et al. 2024, *ApJL*, 960, L1, doi: [10.3847/2041-8213/ad0e76](https://doi.org/10.3847/2041-8213/ad0e76)
- Niida, M., Nagao, T., Ikeda, H., et al. 2020, *ApJ*, 904, 89, doi: [10.3847/1538-4357/abbe11](https://doi.org/10.3847/1538-4357/abbe11)
- Oesch, P. A., Brammer, G., Naidu, R. P., et al. 2023, arXiv e-prints, arXiv:2304.02026, doi: [10.48550/arXiv.2304.02026](https://doi.org/10.48550/arXiv.2304.02026)
- Ono, Y., Harikane, Y., Ouchi, M., et al. 2023, *ApJ*, 951, 72, doi: [10.3847/1538-4357/acd44a](https://doi.org/10.3847/1538-4357/acd44a)
- Onoue, M., Inayoshi, K., Ding, X., et al. 2023, *ApJL*, 942, L17, doi: [10.3847/2041-8213/aca9d3](https://doi.org/10.3847/2041-8213/aca9d3)
- Pacucci, F., & Loeb, A. 2024, *ApJ*, 964, 154, doi: [10.3847/1538-4357/ad3044](https://doi.org/10.3847/1538-4357/ad3044)
- Pacucci, F., & Narayan, R. 2024, arXiv e-prints, arXiv:2407.15915, doi: [10.48550/arXiv.2407.15915](https://doi.org/10.48550/arXiv.2407.15915)
- Parkinson, H., Cole, S., & Helly, J. 2008, *MNRAS*, 383, 557, doi: [10.1111/j.1365-2966.2007.12517.x](https://doi.org/10.1111/j.1365-2966.2007.12517.x)
- Pérez-González, P. G., Barro, G., Rieke, G. H., et al. 2024, *ApJ*, 968, 4, doi: [10.3847/1538-4357/ad38bb](https://doi.org/10.3847/1538-4357/ad38bb)
- Pezzulli, E., Valiante, R., & Schneider, R. 2016, *MNRAS*, 458, 3047, doi: [10.1093/mnras/stw505](https://doi.org/10.1093/mnras/stw505)
- Pizzati, E., Hennawi, J. F., Schaye, J., et al. 2024, arXiv e-prints, arXiv:2403.12140, doi: [10.48550/arXiv.2403.12140](https://doi.org/10.48550/arXiv.2403.12140)

- Regan, J. A., Downes, T. P., Volonteri, M., et al. 2019, *MNRAS*, 486, 3892, doi: [10.1093/mnras/stz1045](https://doi.org/10.1093/mnras/stz1045)
- Reines, A. E., & Volonteri, M. 2015, *ApJ*, 813, 82, doi: [10.1088/0004-637X/813/2/82](https://doi.org/10.1088/0004-637X/813/2/82)
- Sassano, F., Capelo, P. R., Mayer, L., Schneider, R., & Valiante, R. 2023, *MNRAS*, 519, 1837, doi: [10.1093/mnras/stac3608](https://doi.org/10.1093/mnras/stac3608)
- Sassano, F., Schneider, R., Valiante, R., et al. 2021, *MNRAS*, 506, 613, doi: [10.1093/mnras/stab1737](https://doi.org/10.1093/mnras/stab1737)
- Schneider, R., Valiante, R., Trinca, A., et al. 2023, *MNRAS*, 526, 3250, doi: [10.1093/mnras/stad2503](https://doi.org/10.1093/mnras/stad2503)
- Scholtz, J., Maiolino, R., D'Eugenio, F., et al. 2023, arXiv e-prints, arXiv:2311.18731, doi: [10.48550/arXiv.2311.18731](https://doi.org/10.48550/arXiv.2311.18731)
- Shakura, N. I., & Sunyaev, R. A. 1973, *A&A*, 500, 33
- Shen, X., Hopkins, P. F., Faucher-Giguère, C.-A., et al. 2020, *MNRAS*, 495, 3252, doi: [10.1093/mnras/staa1381](https://doi.org/10.1093/mnras/staa1381)
- Shi, Y., Kremer, K., & Hopkins, P. F. 2024, *ApJL*, 969, L31, doi: [10.3847/2041-8213/ad5a95](https://doi.org/10.3847/2041-8213/ad5a95)
- Smith, B. D., Regan, J. A., Downes, T. P., et al. 2018, *MNRAS*, 480, 3762, doi: [10.1093/mnras/sty2103](https://doi.org/10.1093/mnras/sty2103)
- Stern, J., & Laor, A. 2012, *MNRAS*, 423, 600, doi: [10.1111/j.1365-2966.2012.20901.x](https://doi.org/10.1111/j.1365-2966.2012.20901.x)
- Suh, H., Scharwächter, J., Farina, E. P., et al. 2024, arXiv e-prints, arXiv:2405.05333, doi: [10.48550/arXiv.2405.05333](https://doi.org/10.48550/arXiv.2405.05333)
- Tanaka, T., & Haiman, Z. 2009, *ApJ*, 696, 1798, doi: [10.1088/0004-637X/696/2/1798](https://doi.org/10.1088/0004-637X/696/2/1798)
- Tang, J.-J., Goto, T., Ohya, Y., et al. 2019, *MNRAS*, 484, 2575, doi: [10.1093/mnras/stz134](https://doi.org/10.1093/mnras/stz134)
- Taylor, A. J., Finkelstein, S. L., Kocevski, D. D., et al. 2024, arXiv e-prints, arXiv:2409.06772, doi: [10.48550/arXiv.2409.06772](https://doi.org/10.48550/arXiv.2409.06772)
- Tortosa, A., Ricci, C., Ho, L. C., et al. 2023, *MNRAS*, 519, 6267, doi: [10.1093/mnras/stac3590](https://doi.org/10.1093/mnras/stac3590)
- Trinca, A., Schneider, R., Maiolino, R., et al. 2023, *MNRAS*, 519, 4753, doi: [10.1093/mnras/stac3768](https://doi.org/10.1093/mnras/stac3768)
- Trinca, A., Schneider, R., Valiante, R., et al. 2024, *MNRAS*, 529, 3563, doi: [10.1093/mnras/stae651](https://doi.org/10.1093/mnras/stae651)
- . 2022, *MNRAS*, 511, 616, doi: [10.1093/mnras/stac062](https://doi.org/10.1093/mnras/stac062)
- Übler, H., Maiolino, R., Curtis-Lake, E., et al. 2023, arXiv e-prints, arXiv:2302.06647, doi: [10.48550/arXiv.2302.06647](https://doi.org/10.48550/arXiv.2302.06647)
- Valiante, R., Schneider, R., Graziani, L., & Zappacosta, L. 2018a, *MNRAS*, 474, 3825, doi: [10.1093/mnras/stx3028](https://doi.org/10.1093/mnras/stx3028)
- Valiante, R., Schneider, R., Volonteri, M., & Omukai, K. 2016, *Monthly Notices of the Royal Astronomical Society*, 457, 3356
- Valiante, R., Schneider, R., Zappacosta, L., et al. 2018b, *MNRAS*, 476, 407, doi: [10.1093/mnras/sty213](https://doi.org/10.1093/mnras/sty213)
- Volonteri, M., Habouzit, M., & Colpi, M. 2023, *MNRAS*, 521, 241, doi: [10.1093/mnras/stad499](https://doi.org/10.1093/mnras/stad499)
- Volonteri, M., Trebitsch, M., Dubois, Y., et al. 2024, arXiv e-prints, arXiv:2408.12854, doi: [10.48550/arXiv.2408.12854](https://doi.org/10.48550/arXiv.2408.12854)
- Williams, C. C., Tacchella, S., Maseda, M. V., et al. 2023, *ApJS*, 268, 64, doi: [10.3847/1538-4365/acf130](https://doi.org/10.3847/1538-4365/acf130)
- Yang, G., Caputi, K. I., Papovich, C., et al. 2023, *ApJL*, 950, L5, doi: [10.3847/2041-8213/acd639](https://doi.org/10.3847/2041-8213/acd639)
- Yue, M., Eilers, A.-C., Ananna, T. T., et al. 2024a, *ApJL*, 974, L26, doi: [10.3847/2041-8213/ad7eba](https://doi.org/10.3847/2041-8213/ad7eba)
- Yue, M., Eilers, A.-C., Simcoe, R. A., et al. 2024b, *ApJ*, 966, 176, doi: [10.3847/1538-4357/ad3914](https://doi.org/10.3847/1538-4357/ad3914)
- Zappacosta, L., Piconcelli, E., Giustini, M., et al. 2020, *A&A*, 635, L5, doi: [10.1051/0004-6361/201937292](https://doi.org/10.1051/0004-6361/201937292)
- Zappacosta, L., Piconcelli, E., Fiore, F., et al. 2023, *A&A*, 678, A201, doi: [10.1051/0004-6361/202346795](https://doi.org/10.1051/0004-6361/202346795)
- Zhang, Y., Ouchi, M., Gebhardt, K., et al. 2023, *ApJ*, 948, 103, doi: [10.3847/1538-4357/acc2c2](https://doi.org/10.3847/1538-4357/acc2c2)